Role of muscle forces on strain distributions in the proximal femur

Michael P. Rogalski[a], Saulo Martelli[b], Marcus G. Pandy[c], Mariana E. Kersh[a,d,e,*]

[a]*Department of Mechanical Science and Engineering The Grainger College of Engineering, University of Illinois Urbana-Champaign*
[b]*Queendland University of Technology*
[c]*Department of Mechanical Engineering, University of Melbourne*
[d]*Beckman Institute for Advanced Science and Technology, University of Illinois Urbana-Champaign*
[e]*Carle Illinois College of Medicine, University of Illinois Urbana-Champaign*

Abstract

Despite the benefits of exercise for bone health, the development of protocols to improve bone quality in fracture prone areas remains a challenge because of the difficulty in determining how bone is loaded *in vivo*. Discussions persist regarding whether the femoral neck is in bending or compression and the degree to which muscle forces contribute to loading. We simulated the loads during walking using subject-specific muscle-driven finite element models and compared three loading configurations: [1] all hip-spanning muscle and joint forces, [2] a sub-set of hip muscle and joint forces, and [3] hip joint forces only. We found that the use of the hip joint contact force alone resulted in large tensile and compressive principal strains. However, including muscle forces resulted in significantly decreased strain magnitudes and a change of mode to uneven compression in the femoral neck suggesting that the inclusion of muscle forces offset the bending moment observed in a hip-joint-force-only model. In the pertrochanter, including hip muscle forces increased the compressive and tensile strains. Together, these findings indicate that including hip-spanning muscle forces changes the mode and distributions of strains in the femoral neck as well as strain magnitudes in the pertrochanter. Future studies will benefit from including both muscle and joint reaction forces in simulations of bone under *in vivo* loading conditions in order to develop informed exercise interventions to improve bone health.

Keywords: Bone, ground reaction forces, equine biomechanics, analytical model, growth

1. Introduction

Exercise has been shown to be an inexpensive and promising means for encouraging bone adaptation Fuchs et al. (2001), MacKelvie et al. (2001), Petit et al. (2002), Lang et al. (2014), Nikander et al. (2009) and is most effective when the loads incurred are different from those expected during everyday activities. Unfortunately, targeted adaptation of the femoral neck, a region prone to fracture following a fall, has been less successful with variable results reported in exercise-induced adaptation Lang et al. (2014), Nikander et al. (2009). In order to identify activities that encourage bone adaptation and mitigate femoral neck fractures, it is critical to first understand femoral neck loading during regular activity and quantify the resulting mechanical environment Kersh et al. (2018).

One of the first studies on daily loading of the femoral neck was by Julius Wolff in 1892 Wolff (1893, 1986) in which he posited two theories related to bone adaptation: (1) Wolff's Law of

*Corresponding author
Email address: mkersh@illinois.edu (Mariana E. Kersh)

bone formation, which suggests that bone will adapt in response to the forces applied and (2) Wolff's Trajectorial Theory. The latter, founded on Ward's and Von Meyer's models, was based on modeling the femur as a curved cantilever beam with only the hip joint force acting at the femoral head. This loading results in bending with compression on the medial/inferior side of the femoral neck and tension on the lateral/superior side. Wolff supported the Trajectorial Theory by referring to the bending caused by the neck shaft angle and most famously, that the trabecular structures in the femoral neck aligned with the tensile and compressive stresses Wolff (1893, 1986), Hammer (2015).

However, the mechanical state of physiologically loaded bone, and its consequence on adaptation, has since been re-evaluated. Taylor and colleagues first demonstrated that the diaphysis of the femur is predominantly loaded in compression and not bending when muscle forces are included in finite element (FE) simulations Taylor et al. (1996). Using numerical models, Duda et al added evidence that muscle forces play a substantial role in balancing loads in the femur diaphysis and trochanter and that bending moments decreased when muscle forces were included Duda et al. (1997, 1998).

Rudman and colleagues used a 2D plane stress FE model to show that there are predominantly compressive stresses in the proximal femur when capsular ligament forces were included Rudman et al. (2006). These computational findings are supported by Simoes et al, who showed experimentally using strain gauges placed along a synthetic femur that strains decreased when both muscle forces and the hip joint reaction force were applied in contrast to application of the hip force alone Simões et al. (2000).

Despite the evidence indicating that muscle forces change the strain state and magnitudes of the femur, the inclusion of muscles forces in models of physiological activities is limited. Often, the rationale for this simplification is that muscle forces are difficult to quantify and apply experimentally or computationally. Of the 22 muscles that span the hip, an analysis of their contribution to femoral neck loads indicates that 3 muscles (gluteus medius, gluteus minimus, and the iliopsoas) account for more than 90% of the strain in the femoral neck Kersh et al. (2018). However, their contribution to femoral neck loading compared to the hip joint reaction force alone was not evaluated.

To our knowledge, no study has directly compared the strain distributions between subject-specific femoral FE models with and without muscle forces. Thus, it remains unclear whether including muscle forces results in significant differences in femoral neck strains during physiological tasks such as walking. Understanding whether muscle forces influence the strain state of the proximal femur is needed to justify the expense and effort of including muscle forces in computational predictions of bone mechanics during physiological tasks.

Therefore, the aim of this study was to use 3D subject-specific finite-element models to compare principal strains and their orientations during walking for three loading configurations: [1] hip joint force and all hip-spanning muscles, [2] hip joint force and muscles forces from gluteus medius, gluteus minimus, and the iliopsoas, and [3] hip joint force only. Strain was computed because it has been suggested as a likely mechanical stimulus for bone (re)modeling Frost (1983, 2001), Mullender and Huiskes (1995), Goodship et al. (1979), Lanyon and Baggott (1976). Principal orientation was computed as an indicator of trabecular bone orientation Ryan and Ketcham (2005), Martin et al. (2015), Biewener et al. (1996), TOBIN (1955) and patterns of mechanoadaptation Verhulp et al. (2008). The principal strains and their orientations were compared in 20 regions of the proximal femur. We hypothesized that the model with the hip contact force and all muscle forces would have the lowest principal strains and different principal strain orientations compared to the model with hip contact force only.

2. Materials and Methods

2.1. Gait Experiments, Computed Tomography Imaging, and Musculoskeletal Modeling

A subset of data (n=20) from a previously published study were analyzed Kersh et al. (2018). To summarize, postmenopausal women (ages 60-74 years) with no history of lower-extremity fractures, drug therapy, and musculoskeletal disease were asked to walk at a self-selected speed. Kinematic and ground reaction force data were collected using a nine-camera motion capture system and three in-ground force plates, respectively. A generic musculoskeletal model (OpenSim) Delp et al. (2007) was scaled to each participant and inverse kinematic analysis was used to calculate the joint angles, which were then combined with ground reaction force data to calculate the joint torques using inverse dynamics. Static optimization was used to calculate muscle forces and verified against electromyographic data recorded for a subset of lower-limb muscles. Computed tomography (CT) images of the lower limbs were acquired with an isotropic voxel size of 0.5mm, and a calibration phantom was used to convert CT attenuation data into apparent Young's modulus.

2.2. Finite Element Modeling

The femur was segmented from the CT images (Amira v5.3; Thermo Scientific, Hillsboro, OR, USA) and discretized into quadratic tetrahedral elements (Abaqus v6.11; Simulia, Paris, France). The FE model assumed spatially heterogeneous, isotropic Young's moduli and a Poisson's ratio of 0.3 Wallace (2013), Wirtz et al. (2000). The hip joint force was applied as a point vector on the femoral head and muscle forces were applied at the node closest to the muscle attachment point and oriented along the muscle force line-of-action. The distal end of the femur was constrained against all displacements, and axial springs were applied to the femoral head to represent the hip capsule.

We developed three different models from these data: Load 1 - JRF+all hip spanning muscles: hip joint contact force, gluteus medius, gluteus maximus, gluteus minimus, iliopsoas, and several other smaller hip spanning muscles, Load 2 - JRF+some hip spanning muscles: hip joint contact force, gluteus medius, gluteus minimus, and the iliopsoas, and Load 3 - JRF only: hip joint contact force only (Table S1). The lateral/superior, medial/inferior, anterior, and posterior quadrants of 5 regions (proximal femoral neck, middle femoral neck, distal femoral neck, pertrochanter, subtrochanter) were identified based on anatomical landmarks (Fig. 1A).

2.3. Principal Strain and Principal Orientation Calculations

The time point corresponding to maximum strains during the first half of the stance phase Kersh et al. (2018) was used to calculate the element-wise principal strains and orientations in MATLAB (vR2018b; MathWorks, Natick, MA, USA). First, elements with Young's moduli below 1000 MPa Novitskaya et al. (2011) were assumed to correspond to bone marrow and were removed from the analysis. The strain tensor for each remaining element was assembled according to Equation 1:

$$\varepsilon_{ij} = \begin{bmatrix} \varepsilon_{11} & \varepsilon_{12} & \varepsilon_{13} \\ \varepsilon_{21} & \varepsilon_{22} & \varepsilon_{23} \\ \varepsilon_{31} & \varepsilon_{32} & \varepsilon_{33} \end{bmatrix} \tag{1}$$

where ε_{ij} is the strain in each coordinate direction.

Next, the maximum (ϵ_1) and minimum (ϵ_3) principal strains were calculated according to Equations 2, 3 and 4:

$$Det\left|\varepsilon_{ij} - \lambda I\right| = 0 \tag{2}$$

$$\varepsilon_1 = max\left(\lambda_1, \lambda_2, \lambda_3\right) \tag{3}$$

$$\varepsilon_3 = min\left(\lambda_1, \lambda_2, \lambda_3\right) \tag{4}$$

where $\left(\lambda_1, \lambda_2, \lambda_3\right)$ are the eigenvalues of the strain tensor and I is the identity matrix.

For each subject, the elements corresponding to the median and 95th percentile principal

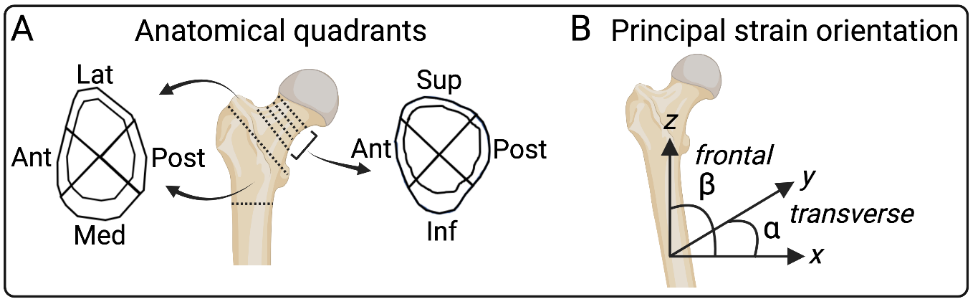

Figure 1: Subject-specific (n=20) FE models were divided into three regions along the femoral neck and two in the trochanter. Each region was further subdivided into anatomical quadrants (Lat=lateral, Ant=anterior, Post=posterior, Med=medial, Sup=superior, Inf=inferior) (A). Principal strains and orientations (B) were calculated within each anatomical quadrant.

strain in each region of the proximal femur were identified. The median principal strain of all twenty subjects was then calculated for each region and for all three loading conditions. In this study, maximum and minimum principal strains are synonymous with tensile and compressive strains, respectively.

We calculated the principal strain orientation (v) using the eigenvector (λ) corresponding to the tensile and compressive principal strains (Equations 5,6):

$$\left|\varepsilon_{ij} - \lambda I\right| v = 0 \tag{5}$$

$$v = \begin{bmatrix} v_x & v_y & v_z \end{bmatrix} \tag{6}$$

The x, y, and z directions of the principal orientation vector correspond to the medial, posterior, and proximal anatomical directions in the FE model, respectively. The vector components were then used to calculate two orientation angles: alpha (y/x, in the transverse plane) and beta (z/x, in the coronal/frontal plane) (Fig. 1B).

2.4. Statistical Analysis

Normality was checked using the Kolmogorov-Smirnov test and because all data were found to be non-normally distributed, the results are presented as medians and median absolute deviations. We compared the "all muscle" group (Load 1) to the remaining two load groups (Load 2 and 3) using a linear mixed-effects model (Equation 7) at an alpha level of 0.05.

$$MechVariable \sim Condition + \left(1 \mid Subject\right) \tag{7}$$

where MechVariable corresponds to max/min principal strain or principal orientation, condition is Load 1, 2, or 3, and subject was included as a random variable. All analyses were performed in MATLAB R2018b (MathWorks, Natick, MA, USA).

3. Results

For all analyses, the maximum principal strains were in tension and minimum principal strains were in compression. These values are herein referred to as the median tensile and compressive strains, respectively where median refers to the median of all subjects. Overall, the effect of different loading conditions on the tensile and compressive strains was similar for all three regions of the femoral neck and between the subtrochanter and pertrochanter regions. Here we report the data for the middle femoral neck and pertrochanter. Data for the remaining sections are reported in Supplemental Tables 5 and S3.

3.1. Principal Strain

<u>Overall strain state:</u> Within the femoral neck, the compressive strains during walking were greater in magnitude than the tensile strains for all loading conditions with the exception of the superior neck under Load 3 (Table 1).

Table 1: Median (median absolute deviation) of tensile and compressive microstrains for 3 loading conditions in four quadrants of the middle femoral neck and pertrochanter. *p<0.05, **p<0.01, *** p<0.001

	Median Tensile Strain ($\mu\varepsilon$)			Median Compressive Strain ($\mu\varepsilon$)		
	Load 1: All muscle + JRF	Load 2: Some muscle + JRF	Load 3: JRF only	Load 1: All muscle + JRF	Load 2: Some muscle + JRF	Load 3: JRF only
Middle Neck						
Superior	601 (198)	670 (179)	**1440 (175)*** **	-854 (272)	-845 (251)	**-519 (107)*** **
Posterior	565 (128)	610 (127)	**836 (191)*** **	-1405 (275)	**-1528 (320)***	**-996 (234)*** **
Inferior	516 (94)	**544 (102)***	**679 (113)*** **	-1608 (275)	**-1690 (293)***	**-1989 (316)*** **
Anterior	408 (93)	**469 (130)** **	**662 (118)*** **	-946 (146)	-914 (174)	**-1276 (270)*** **
Pertrochanter						
Lateral	1447 (258)	1424 (240)	**439 (116)*** **	-766 (140)	-766 (119)	**-294 (65)*** **
Posterior	613 (154)	650 (189)	**481 (91)** **	-708 (161)	**-769 (172)***	**-607 (117)*** **
Medial	577 (104)	**645 (76)*** **	**561 (82)** **	-1414 (225)	**-1562 (211)*** **	**-1396 (220)** **
Anterior	856 (240)	**1019 (255)***	**478 (123)*** **	-996 (228)	-1056 (223)	**-581 (108)*** **

When only the joint reaction force was used, the tensile strains in the superior quadrant was larger than the compressive strains (1440 $\mu\varepsilon$ vs -519 $\mu\varepsilon$). For all loading conditions in the pertrochanter, the tensile strains were consistently larger than the compressive strains in the lateral quadrant, and the compressive strains were larger than the tensile strains in the posterior, medial, and anterior quadrants.

As muscle forces were progressively included from Load 3 to 1, the strain range (max - min) in the femoral neck across all four quadrants decreased, resulting in a more homogeneous strain distribution. For example, in the middle femoral neck the range of tensile strains decreased from 778 to 201 to 193 $\mu\varepsilon$ and 1470 to 845 to 754 $\mu\varepsilon$ for compressive strains. Similar decreases in strains were evident from Load 3 to 1 for compressive strains in the pertrochanter (1102 to 796 to 706 $\mu\varepsilon$). However, the pertrochanteric tensile strains became less homogeneous as muscle forces were added (122 to 779 to 870 $\mu\varepsilon$).

Regional effect of including muscles:

Relative to Load 1 (JRF+all muscles), the use of the hip joint reaction force alone (Load 3) increased tensile strains in all four quadrants of the middle neck with the largest increase in the superior quadrant (+140.7%, p<0.001) and the smallest in the inferior quadrant (+25.9%, p<0.001). The use of some muscles + JRF (Load 2) resulted in similar trends in the inferior and anterior quadrants but to a lesser degree with increases of +5.3% (p=0.038) and +20.2% (p=0.009), respectively (Table 1, Fig. 2A).

The effect of muscle forces on compressive strains in the femoral neck was more variable. Models using only the joint reaction force decreased the compressive strains by an average of 35% in the superior and posterior quadrants (p<0.001) and increased compressive strains by 32% in the inferior and anterior quadrants (p<0.001) compared to those models using all forces. Load 2 (some muscles + JRF) increased compressive strains in the posterior and inferior quadrants by an average of 8% (Table 1, Fig. 2).

Within the pertrochanter, both the compressive and tensile strains in all four quadrants were lower in models using only the JRF compared to all loads (p<0.0074, bottom half of Table 1). The lateral quadrant had the largest decrease in tensile and compressive strains, -70.9% and -60.3%, respectively, while the medial quadrant had the smallest decrease (-3% and -2.4%, Fig. 2B). Conversely, including some muscles (Load 2) increased the tensile strains in the medial and anterior quadrants (p<0.015), and increased the compressive strains in the

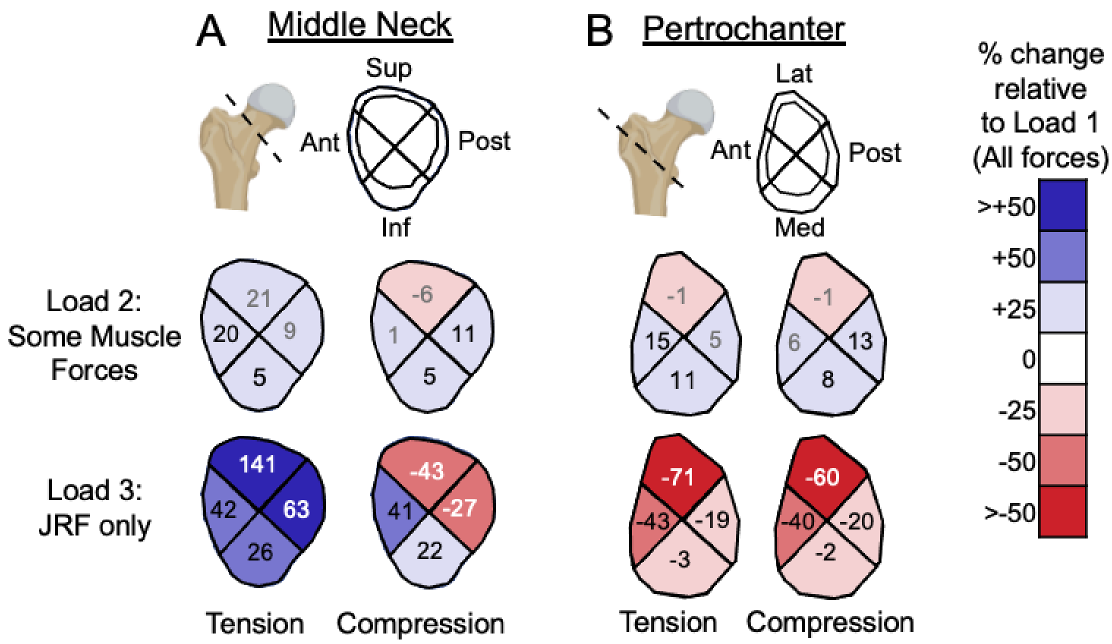

Figure 2: Percent change in loading conditions 2 and 3 relative to loading condition 1 for median tensile and compressive strains in four quadrants of the middle femoral neck (A) and pertrochanter (B). Regions with white or black text were significantly different from Load 1 and gray text was not significantly different.

posterior and medial quadrants ($p<0.038$).

3.2. Principal Orientation

Overall, there was no difference in principal strain orientations in the femoral neck when some muscle forces were used compared to the case when all muscles were applied (Table 2, Fig. 3). The use of the JRF alone shifted the compressive principal strain direction laterally by 62°in the superior quadrant of the mid-femoral neck and 29°in the posterior quadrant ($p=0.004$ and $p<0.001$, respectively) compared to when all loads were included. The tensile strain orientation of the anterior quadrant was also shifted laterally by 141°($p=0.0032$). There were no changes in the orientation of principal strains in the inferior quadrant.

Within the posterior pertrochanter, relative to Load 1, Load 3 shifted the tensile strain orientation laterally by 48°($p<0.001$). In contrast the compressive strain orientation was shifted medially by 59°($p=0.019$) in the posterior quadrant. The use of muscles had a moderate effect on the compressive orientation in the medial quadrant (average of 7.5°medial shift, $p=0.047$ and $p=0.007$). There were no significant changes in the orientation of principal strains in the anterior or lateral quadrants of the pertrochanter.

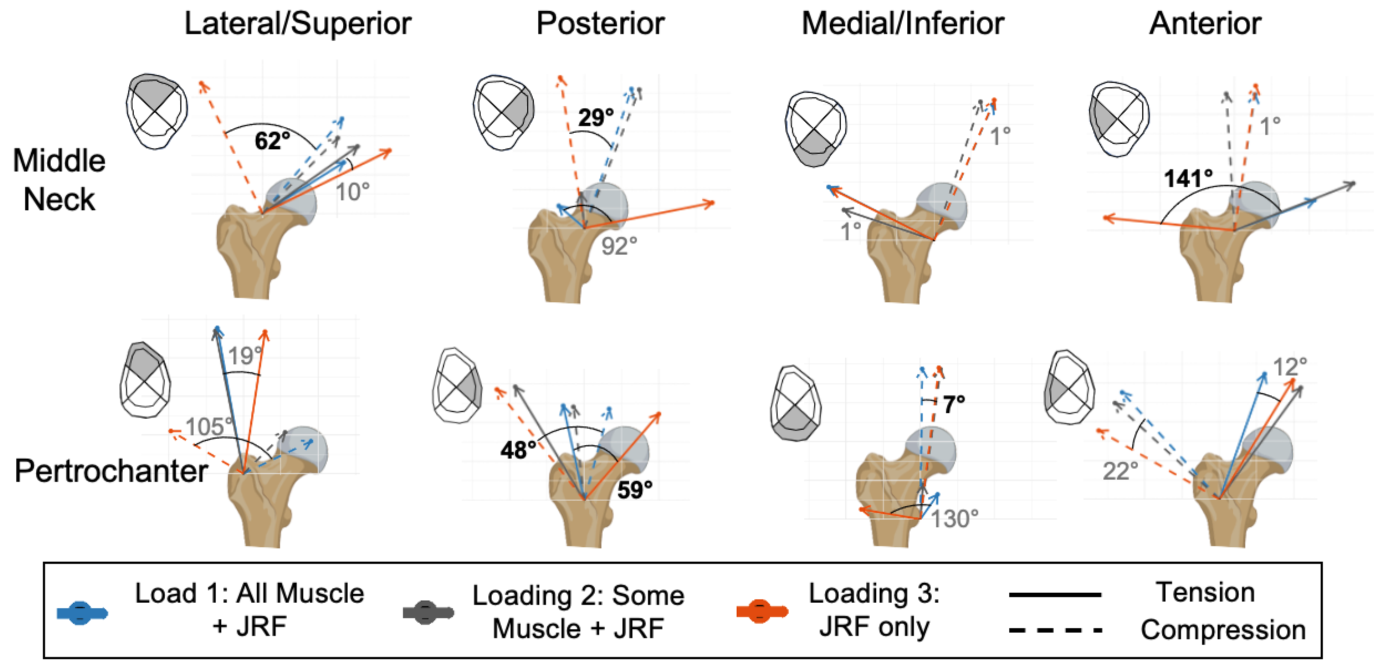

Figure 3: Median compressive and tensile orientation for 3 loading conditions in four quadrants of the middle femoral neck and pertrochanter. Angular values represent differences in principal orientation between Load 1 and 3, where values in black bold were significantly different. Dashed lines denote compressive orientation while solid lines denote tensile orientation.

Table 2: Median (median absolute deviation) of tensile and compressive beta orientation for 3 loading conditions in four quadrants of the middle femoral neck and pertrochanter. Angle of degree 0 is pointing in the medial direction and 180 in the lateral direction. *p<0.05, **p<0.01, *** p<0.001

	Tensile Orientation Beta (°)			Compressive Orientation Beta (°)		
	Load 1: All muscle + JRF	Load 2: Some muscle + JRF	Load 3: JRF only	Load 1: All muscle + JRF	Load 2: Some muscle + JRF	Load 3: JRF only
Middle Neck						
Superior	36.5 (8.7)	39.8 (11.3)	26.7 (6.1)	54.1 (43.2)	47.8 (26)	**116.1 (9.3)****
Posterior	119.9 (57.2)	100.1 (60.3)	27.8 (20.7)	70.5 (11.8)	67.7 (4.8)	**99.5 (3.4)*****
Inferior	152.3 (10)	144.5 (28.6)	153.7 (6.1)	66.2 (10.1)	71.1 (7.1)	65.7 (8.1)
Anterior	25.6 (16.6)	23 (6.6)	**166.5 (9.9)****	80.6 (13.7)	93.3 (13.9)	81.1 (5)
Pertrochanter						
Lateral	100.3 (8.8)	101 (14.6)	81.3 (12.1)	30.2 (20.2)	49.3 (29.2)	134.8 (34.8)
Posterior	100.2 (41)	123.3 (14.6)	**41.2 (20.6)*****	79.9 (44.8)	94.5 (52.3)	**127.5 (20.7)***
Medial	33.1 (28)	104.3 (67.2)	162.7 (13.6)	89.3 (6.1)	**81.9 (5.1)***	**82.8 (5)****
Anterior	67.5 (14.5)	54.3 (8.6)	56 (11.8)	131.5 (10.4)	136.5 (7.6)	153.2 (9.4)

4. Discussion

Our simulations of walking using only the joint reaction force resulted in a state of bending in the femoral neck: the superior neck experienced maximum tensile strains while the inferior neck resulted in maximum compressive strains (Table 1). However, when muscle forces were included (Load 1 and 2), the maximum principal strains of all four quadrants were in compression ($|-\varepsilon_3| > |\varepsilon_1|$), suggesting that including muscle forces decreased the bending moment observed in a hip joint force only model. The shift from bending to uneven compression due to the combined loading of muscle and hip forces is consistent with other studies that have found that the femoral neck is loaded in compression when muscle forces are included Taylor et al. (1996), Duda et al. (1997), Rudman et al. (2006), Sverdlova and Witzel (2010). However, these previous studies did not answer whether the differences were statistically significant since the sample sizes were low (n=1) or model data were derived from different sources.

Our results illustrate that without muscle forces (Load 3), compressive and tensile strains are significantly different in every quadrant from models that include muscle forces. The inclusion of some muscle forces (Load 2) resolves some of the discrepancies, but compressive and tensile strains remained significantly different in the inferior and anterior quadrants of the femoral neck. Likewise, in the pertrochanter the use of the joint reaction force alone resulted in significantly different tensile and compressive strains in every quadrant, and Load 2 had significantly different strains for two quadrants. However, these changes did not alter the balance of tension and compression in the pertrochanter. Compressive strains remained larger than tensile strains for all three models and in every quadrant besides the lateral quadrant, which may be due to the proximity of muscle forces in the pertrochanter.

With decreased bending, and subsequently smaller tensile strains, the models with muscle forces do not follow Wolff's traditional tensile pattern in the femoral neck, supporting other studies that have questioned the validity of the Trajectorial Theory Hammer (2015), Fetto et al. (2002), Skedros and Baucom (2007), Sverdlova (2011). Loading a majority of the trabecular bone in compression makes for better use of the mechanical properties of bone and may be more likely to induce bone remodeling Skedros et al. (2001), Hammer (2015), Morse et al. (2014), Keaveny et al. (2001). Our results contradict the large tensile trajectory in the femoral neck - a central claim of the Trajectorial Theory - but we do not ignore that there remain appreciable tensile strains (Table 1) when muscle forces are included, and some combination of bending and compression in the femoral neck is likely Sverdlova (2011). This is evidenced by the fact that compressive strains were not uniform - and were instead larger in the inferior-posterior quadrants compared to the superior-anterior quadrants.

Including muscle forces also tended to significantly decrease the overall strain magnitudes in the femoral neck, as reported by others when analyzing strains throughout the femur Simões et al. (2000), Ganapathi et al. (2008), Duda et al. (1997). For example, strain gauge measurements of the inferior femoral neck from Simoes and colleagues showed a similar decrease in magnitude ($\approx$ 400 $\mu\varepsilon$) when including muscle forces Simões et al. (2000). According to the mechanostat theory, this decrease may be physiologically significant, as the largest strain value (-1989 $\mu\varepsilon$) in the JRF only model reached the lower limit of the modeling minimum effective strain (MES), which has been proposed to be the threshold which triggers a bone response to reduce strain Frost (1983, 1990). On the other hand, the strain values in the model with muscle forces (-1608 to -854 and 408 to 601 $\mu\varepsilon$) are more consistently within the physiological loading zone defined by the mechanostat theory. The opposite trend is evident in the pertrochanter, wherein strains in this region may be underpredicted (-294 $\mu\varepsilon$) without muscle forces. When muscle forces are included, compressive and tensile strains increase in the pertrochanter and fall within a more physiologically realistic strain range (-1414 to -708 and 577 to 1447 $\mu\varepsilon$, Table 1). Several finite element studies also point to the physiological significance of a homogeneous strain distribution as a result of an optimal distribution of material to sustain mechanical loadsDuda et al. (1998), Sverdlova and Witzel (2010). In our models, when both muscle and the joint reaction force were included, the strain distributions within the femoral neck were more homogeneous.

The strain orientations in the middle neck and pertrochanter were sensitive to muscle forces, but only in certain quadrants (Tables 1, 2). In the femoral neck, the largest changes in orientation occurred in the superior quadrant, while the inferior quadrant saw no change in orientation. These results follow the same pattern as the changes in strain magnitude, potentially indicating a link between loading mode (bending vs. compression) and strain orientation. In the pertrochanter, the largest changes occurred in the posterior and medial quadrants, which did not follow the same pattern as strain magnitude. Both the femoral neck and pertrochanter were more sensitive to changes in their compressive, rather than tensile, orientation. The influence of muscle forces on strain orientation in the proximal femur should not be ignored and may be particularly relevant for studies modelling bone adaptation or investigating trabecular bone orientation.

There are a few limitations to this study. The results shown here may differ for activities other than walking or non-postmenopausal individuals. For higher loading activities, different numerical strain values and trends are likely due to the difference in magnitude and relative contribution of muscle groups Kersh et al. (2018). Another limitation is that our models assumed isotropic Young's moduli. Orthotropic moduli would undoubtedly provide more realistic material properties, but the error due to isotropic moduli is small Peng et al. (2006) and systematic when comparing the three models. Lastly, proximal femur geometry may also contribute to bending. Others have shown that the hip axis length and neck shaft angle is linked to the degree of bending and hip fracture risk Gregory and Aspden (2008), Thevenot et al. (2014), Kazemi et al. (2016), but we do not expect these parameters to affect our results since the role of muscle forces on the same subject was considered.

In conclusion, our findings support the hypothesis that finite element models used to calculate femoral neck strains during walking should not neglect the contribution of muscle forces, as they reduce bending and result in a different strain distribution pattern. While subject specific FE modeling, as done here, is time consuming and not always feasible; the location, direction, and magnitude of muscle forces may be estimated with published data Viceconti et al. (2003), Cristofolini et al. (1995) and would likely yield more physiologically accurate loading of the proximal femur. The introduction of telemetric implants - which provide measures of joint reaction forces in persons following joint arthroplasty - are a valuable source for physiological boundary conditions; however these joint loads measured are a response to muscle forces and therefore only represent a subset of the physiological loads applied to bone. FE models including muscle forces are useful tools for understanding how bone is physiologically loaded during normal activity, which is critical to identify activities that may encourage bone remodeling and prevent femoral neck fractures.

5. Acknowledgments

We would like to thank the Department of Mechanical Science and Engineering for their support of the study through a fellowship and the Velux Foundation.

References

Biewener, A. A.; Fazzalari, N. L.; Konieczynski, D. D., and Baudinette, R. V. Adaptive changes in trabecular architecture in relation to functional strain patterns and disuse. *Bone*, 1996. ISSN 87563282. doi: 10.1016/8756-3282(96)00116-0.

Cristofolini, Luca; Viceconti, Marco; Toni, Aldo, and Giunti, Armando. Influence of thigh muscles on the axial strains in a proximal femur during early stance in gait. *Journal of Biomechanics*, 28(5):617–624, may 1995. ISSN 00219290. doi: 10.1016/0021-9290(94)00106-E. URL https://www.ncbi.nlm.nih.gov/pubmed/7775497http://jbjs.org/article.aspx?doi=10.2106/JBJS.OT.K.00082https://linkinghub.elsevier.com/retrieve/pii/002192909400106E.

Delp, Scott L.; Anderson, Frank C.; Arnold, Allison S.; Loan, Peter; Habib, Ayman; John, Chand T.; Guendelman, Eran, and Thelen, Darryl G. Opensim: Open-source software to create and analyze dynamic simulations of movement. *IEEE Transactions on Biomedical Engineering*, 54(11):1940–1950, 2007. doi: 10.1109/TBME.2007.901024.

Duda, Georg N.; Schneider, Erich, and Chao, Edmund Y.S. Internal forces and moments in the femur during walking. *Journal of Biomechanics*, 1997. ISSN 00219290. doi: 10.1016/S0021-9290(97)00057-2.

Duda, Georg N.; Heller, Markus; Albinger, Juergen; Schulz, Olaf; Schneider, Erich, and Claes, Lutz. Influence of muscle forces on femoral strain distribution. *Journal of Biomechanics*, 1998. ISSN 00219290. doi: 10.1016/S0021-9290(98)00080-3.

Fetto, Joseph; Leali, Alex, and Moroz, Alex. Evolution of the Koch model of the biomechanics of the hip: Clinical perspective, 2002. ISSN 09492658.

Frost, H. M. A determinant of bone architecture. The minimum effective strain. *Clinical Orthopaedics and Related Research*, 1983. ISSN 0009921X. doi: 10.1097/00003086-198305000-00047.

Frost, H. M. Skeletal structural adaptations to mechanical usage (SATMU): 1. Redefining Wolff's Law: The bone modeling problem. *The Anatomical Record*, 1990. ISSN 10970185. doi: 10.1002/ar.1092260402.

Frost, Harold M. From Wolff's law to the Utah paradigm: Insights about bone physiology and its clinical applications, 2001. ISSN 0003276X.

Fuchs, R. K.; Bauer, J. J., and Snow, C. M. Jumping improves hip and lumbar spine bone mass in prepubescent children: A randomized controlled trial. *Journal of Bone and Mineral Research*, 16(1):148–156, 2001. ISSN 08840431. doi: 10.1359/jbmr.2001.16.1.148.

Ganapathi, Muthu; Evans, S., and Roberts, P. Strain pattern following surface replacement of the hip. *Proceedings of the Institution of Mechanical Engineers, Part H: Journal of Engineering in Medicine*, 2008. ISSN 09544119. doi: 10.1243/09544119JEIM322.

Goodship, A. E.; Lanyon, L. E., and McFie, H. Functional adaptation of bone to increased stress. An experimental study. *Journal of Bone and Joint Surgery - Series A*, 1979. ISSN 00219355. doi: 10.2106/00004623-197961040-00008.

Gregory, Jennifer S. and Aspden, Richard M. Femoral geometry as a risk factor for osteoporotic hip fracture in men and women, 2008. ISSN 13504533.

Hammer, A. The paradox of Wolff's theories, 2015. ISSN 18634362.

Kazemi, Seyyed Morteza; Qoreishy, Mohamad; Keipourfard, Ali; Sajjadi, Mohammadreza Minator, and Shokraneh, Shahram. Effects of hip geometry on fracture patterns of proximal femur. *Archives of Bone and Joint Surgery*, 2016. ISSN 2345461X. doi: 10.22038/abjs.2016.6993.

Keaveny, T. M.; Morgan, E. F.; Niebur, G. L., and Yeh, O. C. Biomechanics of trabecular bone, 2001. ISSN 15239829.

Kersh, Mariana E.; Martelli, Saulo; Zebaze, Roger; Seeman, Ego, and Pandy, Marcus G. Mechanical Loading of the Femoral Neck in Human Locomotion. *Journal of Bone and Mineral Research*, 33(11):1999–2006, 2018. ISSN 15234681. doi: 10.1002/jbmr.3529.

Lang, Thomas F.; Saeed, Isra H.; Streeper, Timothy; Carballido-Gamio, Julio; Harnish, Roy J.; Frassetto, Lynda A.; Lee, Stuart M.C.; Sibonga, Jean D.; Keyak, Joyce H.; Spiering, Barry A.; Grodsinsky, Carlos M.; Bloomberg, Jacob J., and Cavanagh, Peter R. Spatial heterogeneity in the response of the proximal femur to two lower-body resistance exercise regimens. *Journal of Bone and Mineral Research*, 29(6):1337–1345, 2014. ISSN 15234681. doi: 10.1002/jbmr.2155.

Lanyon, L. E. and Baggott, D. G. Mechanical function as an influence on the structure and form of bone. *Journal of Bone and Joint Surgery - Series B*, 1976. ISSN 0301620X. doi: 10.1302/0301-620x.58b4.1018029.

MacKelvie, Kerry J.; McKay, Heather A.; Khan, Karim M., and Crocker, Peter R.E. A school-based exercise intervention augments bone mineral accrual in early pubertal girls. *Journal of Pediatrics*, 139(4):501–508, 2001. ISSN 00223476. doi: 10.1067/mpd.2001.118190.

Martin, R. Bruce; Burr, David B.; Sharkey, Neil A., and Fyhrie, David P. *Skeletal Tissue Mechanics*. 2015. doi: 10.1007/978-1-4939-3002-9.

Morse, Alyson; McDonald, Michelle Maree; Kelly, Natalie H.; Melville, Katherine M.; Schindeler, Aaron; Kramer, Ina; Kneissel, Michaela; Van Der Meulen, Marjolein C.H., and Little, David Graham. Mechanical load increases in bone formation via a Sclerostin-independent pathway. *Journal of Bone and Mineral Research*, 2014. ISSN 15234681. doi: 10.1002/jbmr.2278.

Mullender, M. G. and Huiskes, R. Proposal for the regulatory mechanism of Wolff's law. *Journal of Orthopaedic Research*, 1995. ISSN 1554527X. doi: 10.1002/jor.1100130405.

Nikander, R.; Kannus, P.; Dastidar, P.; Hannula, M.; Harrison, L.; Cervinka, T.; Narra, N. G.; Aktour, R.; Arola, T.; Eskola, H.; Soimakallio, S.; Heinonen, A.; Hyttinen, J., and Sievänen, H. Targeted exercises against hip fragility. *Osteoporosis International*, 20(8): 1321–1328, 2009. ISSN 0937941X. doi: 10.1007/s00198-008-0785-x.

Novitskaya, Ekaterina; Chen, Po-Yu; Hamed, Elham; Jun, Li; Lubarda, Vlado; Jasiuk, Iwona, and Mckittrick, Joanna. Recent advances on the measurement and calculation of the elastic moduli of cortical and trabecular bone: A review. *Theoretical and Applied Mechanics*, 2011. ISSN 1450-5584. doi: 10.2298/tam1103209n.

Peng, Liang; Bai, Jing; Zeng, Xiaoli, and Zhou, Yongxin. Comparison of isotropic and orthotropic material property assignments on femoral finite element models under two loading conditions. *Medical Engineering and Physics*, 2006. ISSN 13504533. doi: 10.1016/j.medengphy.2005.06.003.

Petit, M. A.; McKay, H. A.; Mackelvie, K. J.; Heinonen, A.; Khan, K. M., and Beck, T. J. A randomized school-based jumping intervention confers site and maturity-specific benefits on bone structural properties in girls: A hip structural analysis study. *Journal of Bone and Mineral Research*, 2002. ISSN 08840431. doi: 10.1359/jbmr.2002.17.3.363.

Rudman, K. E.; Aspden, R. M., and Meakin, J. R. Compression or tension? The stress distribution in the proximal femur. *BioMedical Engineering Online*, 2006. ISSN 1475925X. doi: 10.1186/1475-925X-5-12.

Ryan, Timothy M. and Ketcham, Richard A. Angular orientation of trabecular bone in the femoral head and its relationship to hip joint loads in leaping primates. *Journal of Morphology*, 2005. ISSN 03622525. doi: 10.1002/jmor.10315.

Simões, J. A.; Vaz, M. A.; Blatcher, S., and Taylor, M. Influence of head constraint and muscle forces on the strain distribution within the intact femur. *Medical Engineering and Physics*, 22(7):453–459, 2000. ISSN 13504533. doi: 10.1016/S1350-4533(00)00056-4.

Skedros, John G. and Baucom, Sidney L. Mathematical analysis of trabecular 'trajectories' in apparent trajectorial structures: The unfortunate historical emphasis on the human proximal femur. *Journal of Theoretical Biology*, 2007. ISSN 00225193. doi: 10.1016/j.jtbi.2006.06.029.

Skedros, John G.; Mason, Mark W., and Bloebaum, Roy D. Modeling and remodeling in a developing artiodactyl calcaneus: A model for evaluating Frost's mechanostat hypothesis and its corollaries. *Anatomical Record*, 2001. ISSN 0003276X. doi: 10.1002/ar.1094.

Sverdlova, N. Tensile trabeculae - Myth or reality?, 2011. ISSN 11087161.

Sverdlova, Nina S. and Witzel, Ulrich. Principles of determination and verification of muscle forces in the human musculoskeletal system: Muscle forces to minimise bending stress, 2010. ISSN 00219290.

Taylor, M; Tanner, K; Freeman, M, and Yettram, A. Stress and strain distribution within the intact femur: compression or bending? [see comments.]. Comment in: Med Eng Phys. 1997 Jan;19(1):97, 99-100 ; 9140878. *Medical Engineering Physics*, 18(2):122–131, 1996.

Thevenot, Jérome; Hirvasniemi, Jukka; Pulkkinen, Pasi; Maäta, Mikko; Korpelainen, Raija; Saarakkala, Simo, and Jamsä, Timo. Assessment of risk of femoral neck fracture with radiographic texture parameters: A Retrospective study. *Radiology*, 2014. ISSN 15271315. doi: 10.1148/radiol.14131390.

TOBIN, W. J. The internal architecture of the femur and its clinical significance; the upper end. *The Journal of bone and joint surgery. American volume*, 1955. ISSN 00219355. doi: 10.2106/00004623-195537010-00007.

Verhulp, E.; van Rietbergen, B., and Huiskes, R. Load distribution in the healthy and osteoporotic human proximal femur during a fall to the side. *Bone*, 2008. ISSN 87563282. doi: 10.1016/j.bone.2007.08.039.

Viceconti, M.; Ansaloni, M.; Baleani, M., and Toni, A. The muscle standardized femur: A step forward in the replication of numerical studies in biomechanics. *Proceedings of the Institution of Mechanical Engineers, Part H: Journal of Engineering in Medicine*, 217(2): 105–110, 2003. ISSN 09544119. doi: 10.1243/09544110360579312.

Wallace, Joseph M. Skeletal Hard Tissue Biomechanics. In *Basic and Applied Bone Biology*. 2013. ISBN 9780124160156. doi: 10.1016/B978-0-12-416015-6.00006-X.

Wirtz, Dieter Christian; Schiffers, Norbert; Forst, Raimund; Pandorf, Thomas; Weichert, Dieter, and Radermacher, Klaus. Critical evaluation of known bone material properties to realize anisotropic FE-simulation of the proximal femur. *Journal of Biomechanics*, 2000. ISSN 00219290. doi: 10.1016/S0021-9290(00)00069-5.

Wolff, Julius. Das Gesetz der Transformation der Knochen. *Deutsche Medizinische Wochenschrift*, 1893. ISSN 14394413. doi: 10.1055/s-0028-1144106.

Wolff, Julius. *The Law of Bone Remodelling*. 1986. doi: 10.1007/978-3-642-71031-5.

Supplemental Data

Table S1: Loading conditions used to evaluate contributions of muscle forces to principal strains in the proximal femur.

	Load 1	Load 2	Load 3
Joint reaction force	✓	✓	✓
Gluteus medius	✓	✓	
Gluteus minimus	✓	✓	
Iliopsoas (psoas, iliacus)	✓	✓	
Gluteus maximus	✓		
Adductors (brevis, longus, magnus)	✓		
Quadratus femoris	✓		
Vastus medialis, lateralis and intermedius	✓		
Biceps femoris short	✓		
Gemelli	✓		
Pectineus	✓		
Piriformis	✓		

Table S2: Median (median absolute deviation) of tensile and compressive microstrains for 3 loading conditions in four quadrants of the proximal neck, middle neck, distal neck, pertrochanter and subtrochanter. *p<0.05, **p<0.01, *** p<0.001

		Median Tensile Strain ($\mu\varepsilon$)			Median Compressive Strain ($\mu\varepsilon$)		
		Load 1: All muscle + JRF	Load 2: Some muscle + JRF	Load 3: JRF only	Load 1: All muscle + JRF	Load 2: Some muscle + JRF	Load 3: JRF only
Proximal Neck							
Superior		639 (138)	702 (145)	**990 (253)*****	-871 (318)	-833 (296)	**-599 (104)*****
	Med % change		9.9	56.2		-1.1	-37.4
Posterior		651 (134)	**725 (172)***	**786 (124)*****	-1556 (224)	**-1672 (221)****	**-1456 (223)*****
	Med % change		9	18.9		6.2	-11.7
Inferior		583 (106)	**655 (134)***	**787 (128)*****	-1679 (317)	-1762 (358)	**-1990 (271)*****
	Med % change		6.9	30.1		3.8	20
Anterior		474 (101)	490 (99)	**893 (114)*****	-909 (207)	-859 (227)	**-1274 (312)*****
	Med % change		0.8	85.7		-2.6	43.2
Middle Neck							
Superior		601 (198)	670 (179)	**1440 (275)*****	-854 (272)	-845 (251)	**-519 (107)*****
	Med % change		20.5	140.7		-6.4	-43.1
Posterior		565 (128)	610 (127)	**836 (191)*****	-1405 (275)	**-1528 (320)***	**-996 (234)*****
	Med % change		9.1	62.5		10.9	-26.9
Inferior		516 (94)	**544 (102)***	**679 (113)*****	-1608 (275)	**-1690 (293)***	**-1989 (316)*****
	Med % change		5.3	25.9		4.7	22.2
Anterior		408 (93)	**469 (130)****	**662 (118)*****	-946 (146)	-914 (174)	**-1276 (270)*****
	Med % change		20.2	41.7		0.7	41.3
Distal Neck							
Superior		657 (128)	714 (134)	**1154 (152)*****	-1247 (242)	-1238 (204)	**-439 (67)*****
	Med % change		6.7	83.7		-4.3	-67.7
Posterior		449 (95)	478 (95)	**621 (188)****	-944 (159)	-987 (193)	**-566 (82)*****
	Med % change		6.8	32		6	-41.8
Inferior		510 (70)	**531 (66)***	**596 (64)*****	-1544 (229)	**-1612 (236)***	**-1750 (241)*****
	Med % change		3.8	13.4		3.8	12.7
Anterior		580 (140)	**800 (197)*****	**369 (66)*****	-1104 (243)	-1113 (259)	**-702 (122)*****
	Med % change		31.4	-43.1		2.9	-35.9
Pertrochanter							
Lateral		1447 (258)	1424 (240)	**439 (116)*****	-766 (140)	-766 (119)	**-294 (65)*****
	Med % change		-1.3	-70.9		-1.4	-60.3
Posterior		613 (154)	650 (189)	**481 (91)****	-708 (161)	**-769 (172)***	**-607 (117)*****
	Med % change		4.8	-19		12.5	-19.8
Medial		577 (104)	**645 (76)*****	**561 (82)****	-1414 (225)	**-1562 (211)*****	**-1396 (220)****
	Med % change		10.8	-3		8.3	-2.4
Anterior		856 (240)	**1019 (255)***	**478 (123)*****	-996 (228)	-1056 (223)	**-581 (108)*****
	Med % change		15.4	-42.6		6.1	-39.7

continued on next page

		Median Tensile Strain ($\mu\varepsilon$)			Median Compressive Strain ($\mu\varepsilon$)		
		Load 1: All muscle + JRF	Load 2: Some muscle + JRF	Load 3: JRF only	Load 1: All muscle + JRF	Load 2: Some muscle + JRF	Load 3: JRF only
Subtrochanter							
Lateral		1369 (321)	1428 (292)	**686 (177)*****	-536 (111)	**-626 (100)***	**-230 (36)*****
	Med % change		2.2	-46		13.5	-52
Posterior		728 (195)	**861 (181)***	**287 (68)*****	-741 (162)	**-895 (169)*****	**-407 (100)*****
	Med % change		11.3	-59.3		26.3	-34.5
Medial		669 (116)	**728 (119)*****	**492 (83)*****	-1737 (289)	**-1943 (311)***	**-1515 (251)*****
	Med % change		11.8	-14.9		6.4	-9.6
Anterior		485 (159)	**702 (180)****	**228 (66)*****	-837 (289)	-895 (231)	**-332 (144)*****
	Med % change		29.6	-54.1		10.6	-53

Table S3: 95th percentile (median absolute deviation) of tensile and compressive microstrains for 3 loading conditions in four quadrants of the proximal neck, middle neck, distal neck, pertrochanter and subtrochanter. *p<0.05, **p<0.01, *** p<0.001

		95% Tensile Strain ($\mu\varepsilon$)			95% Compressive Strain ($\mu\varepsilon$)		
		Load 1: All muscle + JRF	Load 2: Some muscle + JRF	Load 3: JRF only	Load 1: All muscle + JRF	Load 2: Some muscle + JRF	Load 3: JRF only
Proximal Neck							
Superior		853 (151)	1001 (188)	1709 (388)***	-1503 (359)	-1516 (263)	-1285 (201)**
	Med % change		12.5	76.7		3.5	-17.1
Posterior		870 (169)	970 (202)	1210 (264)***	-2158 (364)	-2345 (483)***	-2191 (477)*
	Med % change		7.9	34		7.1	-1.7
Inferior		812 (188)	820 (176)	1051 (153)***	-2232 (416)	-2298 (419)*	-2719 (415)***
	Med % change		5.4	28.7		4.4	24.2
Anterior		693 (139)	764 (117)	1179 (161)***	-1699 (386)	-1645 (334)	-2309 (323)***
	Med % change		1.9	68.9		0.3	33
Middle Neck							
Superior		877 (269)	1042 (291)	2232 (465)***	-1433 (380)	-1268 (290)	-869 (155)***
	Med % change		17.3	126		-4.3	-43.9
Posterior		787 (133)	866 (160)	1458 (395)***	-2025 (268)	-2232 (362)***	-1833 (355)***
	Med % change		9.6	85.7		11.6	-17.4
Inferior		767 (138)	830 (138)**	1038 (116)***	-2219 (286)	-2445 (352)**	-3013 (472)***
	Med % change		7.6	29.3		8.3	28.7
Anterior		695 (139)	791 (187)**	1029 (194)***	-1517 (343)	-1442 (344)	-2140 (380)***
	Med % change		21.9	37.2		-2.1	46.5
Distal Neck							
Superior		1274 (375)	1414 (391)	2007 (355)***	-2372 (439)	-2278 (374)	-725 (105)***
	Med % change		18	75.7		-8.1	-72.5
Posterior		672 (120)	699 (129)	1503 (265)***	-1488 (246)	-1655 (292)*	-1031 (197)***
	Med % change		8.2	126.3		11.2	-36.2
Inferior		765 (123)	831 (110)**	971 (185)***	-2240 (322)	-2461 (343)**	-2921 (512)***
	Med % change		8.7	20.5		7.9	21.9
Anterior		1193 (358)	1410 (379)***	819 (166)***	-1648 (293)	-1671 (315)	-1580 (284)
	Med % change		32.9	-33.1		1.1	3.6
Pertrochanter							
Lateral		2791 (678)	2666 (699)	1123 (217)***	-2019 (628)	-1998 (635)	-542 (116)***
	Med % change		-2.6	-61.4		-0.9	-74.6
Posterior		1491 (321)	1542 (462)	1059 (254)***	-1562 (291)	-1525 (243)	-927 (150)***
	Med % change		-2.1	-30.8		6.1	-34
Medial		908 (89)	1012 (125)**	834 (125)**	-2678 (334)	-2747 (414)**	-2449 (301)***
	Med % change		10.5	-8.8		3.4	-4.5
Anterior		1455 (331)	1577 (391)**	896 (204)***	-1668 (315)	-1751 (266)	-966 (198)***
	Med % change		11.6	-30		2.2	-35

continued on next page

		95% Tensile Strain ($\mu\varepsilon$)			95% Compressive Strain ($\mu\varepsilon$)		
		Load 1: All muscle + JRF	Load 2: Some muscle + JRF	Load 3: JRF only	Load 1: All muscle + JRF	Load 2: Some muscle + JRF	Load 3: JRF only
Subtrochanter							
Lateral		2205 (501)	2175 (442)	1142 (236)***	-805 (142)	-894 (170)	-426 (88)***
	Med % change		-0.4	-41.2		7.3	-43
Posterior		1678 (351)	1603 (366)	651 (219)***	-1359 (231)	-1595 (290)***	-1267 (223)
	Med % change		-1.4	-60.3		22	-0.2
Medial		917 (189)	1041 (199)***	717 (113)***	-2531 (426)	-2706 (503)	-2260 (359)***
	Med % change		11.9	-13.4		4	-11
Anterior		836 (183)	1086 (232)*	537 (140)***	-1725 (224)	-1742 (255)	-1396 (376)***
	Med % change		22.4	-31.8		-1.7	-22.2

Table S4: Median (median absolute deviation) of tensile and compressive alpha orientation for 3 loading conditions in four quadrants of the proximal neck, middle neck, distal neck, pertrochanter, and subtrochanter. *$p<0.05$, **$p<0.01$, *** $p<0.001$

		Tensile Orientation Alpha (°)			Compressive Orientation Alpha (°)		
		Load 1: All muscle + JRF	Load 2: Some muscle + JRF	Load 3: JRF only	Load 1: All muscle + JRF	Load 2: Some muscle + JRF	Load 3: JRF only
Proximal Neck							
Superior		70.5 (13.9)	60.2 (15.5)	149.3 (23.6)	136.9 (19.6)	128.8 (17.6)	**62.4 (10.3)*****
	Med % change		-10	36.5		-11.9	-54.1
Posterior		62.6 (15.4)	55.2 (11.9)	133.5 (43.5)	29.4 (18)	112.4 (50.6)	80.7 (40.3)
	Med % change		-8.2	104.7		20.7	23.2
Inferior		41 (15.9)	43.2 (12.8)	**99.6 (48.9)*****	133 (20.7)	128.1 (13.5)	146.3 (13.8)
	Med % change		20.3	115.5		-6.8	11.9
Anterior		115.8 (45.4)	142.7 (34.9)	154.8 (7.2)	134.3 (17.2)	**112.3 (14.1)*****	**114.1 (7.1)***
	Med % change		-4.5	21.1		-20.2	-9.4
Middle Neck							
Superior		65.4 (24.4)	53.7 (18.8)	**160.7 (8.1)*****	154.9 (13.5)	**129.6 (18.1)***	**99.7 (43)*****
	Med % change		-2.8	133.4		-10.4	-30.1
Posterior		80.3 (10.5)	79.1 (20.4)	**157.3 (10.4)****	152.3 (16.9)	158.6 (11.2)	**75.9 (31.1)****
	Med % change		-1.3	69		3.8	-45.1
Inferior		71 (48.6)	58 (21.1)	129.9 (19.3)	144.1 (17.2)	139.9 (16.2)	148.5 (10.8)
	Med % change		-1.6	64		-2.2	8.2
Anterior		49.9 (25.5)	38.6 (22.5)	**158.3 (10)*****	95.5 (35.4)	83.8 (26.6)	**113.9 (15.8)***
	Med % change		-2.2	72.4		-15.6	6.6
Distal Neck							
Superior		70 (26.9)	67.2 (28)	**152.9 (15.5)***	152.9 (5.2)	145.9 (6.9)	**39.4 (35.1)*****
	Med % change		-1.5	82		-1	-60.5
Posterior		82.8 (7.5)	77.4 (6.3)	**147 (8.3)*****	147.5 (20.5)	139.1 (19.7)	139.7 (35.8)
	Med % change		-2.9	81.3		-0.6	5.1
Inferior		72.6 (46.1)	78.6 (38.2)	71.8 (44.1)	122.8 (27.3)	121 (23)	143.5 (15.1)
	Med % change		-8.5	-4.2		6.4	21
Anterior		142.3 (28.3)	**161.8 (12.4)***	100.3 (27.2)	35.8 (26.2)	29.4 (22)	35.2 (29.5)
	Med % change		7.5	0.9		-26.7	14.8
Pertrochanter							
Lateral		53.7 (28.9)	50.8 (22.2)	**112.4 (29.6)***	122.6 (32.7)	85.5 (38)	114.8 (39.4)
	Med % change		6.4	68.6		-1.3	-13.1
Posterior		71.8 (45.1)	151.8 (22)	76.4 (38.6)	152.9 (16.5)	155.2 (12.6)	142.6 (33.5)
	Med % change		2.4	-7.4		2.6	-7
Medial		69.4 (22.4)	**111.4 (39.9)****	55.8 (20.6)	78.4 (39.9)	**115.5 (30)***	**131.6 (23.2)****
	Med % change		39.5	-8.1		14.6	36
Anterior		123.6 (25.4)	140.7 (19.3)	108.9 (54.2)	160.4 (10.2)	154.4 (18)	152.4 (18.5)
	Med % change		2.1	8.8		-0.4	-6.2
Subtrochanter							
Lateral		57.6 (42.4)	48.9 (19.5)	**155.8 (10.9)*****	113.3 (43.1)	97.4 (23.7)	64.6 (62.5)
	Med % change		-33	182.7		-17.5	-10.1
Posterior		155.9 (9.6)	155.7 (13.4)	111.1 (49.1)	151.1 (21.7)	137.3 (39.1)	52 (50.7)
	Med % change		-2.3	-12.4		-5.7	-27.2
Medial		90.3 (20.5)	98.9 (16.5)	92.7 (33.4)	91.7 (32.2)	91.5 (29.5)	86.1 (63.7)
	Med % change		5.8	-7.3		-1.1	11.5
Anterior		112.1 (46.2)	149.6 (21.9)	90.8 (46.5)	156.4 (11.7)	156 (12.1)	156.1 (18)
	Med % change		2.3	-5.4		-1.6	-1.9

continued on next page

Table S5: Median (median absolute deviation) of tensile and compressive beta orientation for 3 loading conditions in four quadrants of the proximal neck, middle neck, distal neck, pertrochanter, and subtrochanter. *p<0.05, **p<0.01, *** p<0.001

		Tensile Orientation Beta (°)			Compressive Orientation Beta (°)		
		Load 1: All muscle + JRF	Load 2: Some muscle + JRF	Load 3: JRF only	Load 1: All muscle + JRF	Load 2: Some muscle + JRF	Load 3: JRF only
Proximal Neck							
Superior		36.7 (9.2)	43.1 (18.7)	34.1 (19)	65.1 (18.4)	67.3 (10)	**106.3 (8)***
	Med % change		0.8	-26.2		-1	55.3
Posterior		148.6 (22.1)	168.7 (10.5)	164.9 (5.4)	58.7 (9)	64.5 (9.4)	**84.9 (6.3)***
	Med % change		8.2	8.5		0.6	37.1
Inferior		145 (24.5)	149.4 (27.7)	**160.4 (4.7)***	60.7 (14.4)	57.6 (10.4)	64.7 (11.9)
	Med % change		4.9	14.1		-6.8	0.6
Anterior		144.9 (14.2)	152.2 (20.5)	**160.7 (5.6)***	64.1 (7.5)	73.3 (12.5)	**80 (7.2)***
	Med % change		5.1	8.8		5.4	16.4
Middle Neck							
Superior		36.5 (8.7)	39.8 (11.3)	26.7 (6.1)	54.1 (43.2)	47.8 (26)	**116.1 (9.3)****
	Med % change		-4.7	-27.1		21.6	117.3
Posterior		119.9 (57.2)	100.1 (60.3)	27.8 (20.7)	70.5 (11.8)	67.7 (4.8)	**99.5 (3.4)***
	Med % change		-20	-77.4		0.7	42.1
Inferior		152.3 (10)	144.5 (28.6)	153.7 (6.1)	66.2 (10.1)	71.1 (7.1)	65.7 (8.1)
	Med % change		-0.7	1		2	1.1
Anterior		25.6 (16.6)	23 (6.6)	**166.5 (9.9)****	80.6 (13.7)	93.3 (13.9)	81.1 (5)
	Med % change		16.6	93.5		17.3	-0.2
Distal Neck							
Superior		54.6 (24.8)	60.7 (23.2)	34 (9.2)	146.3 (12.5)	141.3 (7.4)	118.7 (8.5)
	Med % change		3.5	-31.4		-5.8	-18.7
Posterior		56.3 (42.7)	44.9 (28)	32.1 (11.6)	61.1 (35.6)	83.6 (37.4)	**116.7 (7.5)****
	Med % change		-21.7	-32.2		-3.3	90.9
Inferior		140.8 (27.5)	136.6 (37.4)	157.5 (14.8)	80.7 (8.8)	78.3 (7.2)	**73.9 (5.4)***
	Med % change		-2.6	8.4		-5.6	-7.6
Anterior		30.3 (7.5)	36.8 (3.8)	**47.9 (17.6)***	120.1 (10.3)	126.6 (10.1)	118.5 (18.8)
	Med % change		30	50.6		2.5	-2.6
Pertrochanter							
Lateral		100.3 (8.8)	101 (14.6)	81.3 (12.1)	30.2 (20.2)	49.3 (29.2)	134.8 (34.8)
	Med % change		-4.4	-14.9		11.3	29.5
Posterior		100.2 (41)	123.3 (14.6)	**41.2 (20.6)***	79.9 (44.8)	94.5 (52.3)	**127.5 (20.7)***
	Med % change		6.3	-55.2		-0.8	58.4
Medial		33.1 (28)	104.3 (67.2)	162.7 (13.6)	89.3 (6.1)	**81.9 (5.1)***	**82.8 (5)****
	Med % change		3.2	47.2		-8.2	-7.3
Anterior		67.5 (14.5)	54.3 (8.6)	56 (11.8)	131.5 (10.4)	136.5 (7.6)	153.2 (9.4)
	Med % change		-2.1	-5.4		0.9	6.5

continued on next page

		Tensile Orientation Beta (°)			Compressive Orientation Beta (°)		
		Load 1: All muscle + JRF	Load 2: Some muscle + JRF	Load 3: JRF only	Load 1: All muscle + JRF	Load 2: Some muscle + JRF	Load 3: JRF only
Proximal Neck							
Subtrochanter							
Lateral		98.8 (6)	100.5 (4.2)	99.9 (2.2)	21.9 (12.1)	54.6 (37)	12 (3.4)
	Med % change		2.4	0.3		49.1	-36.9
Posterior		121.1 (12.8)	131.9 (6.8)	139.7 (27.4)	53.7 (20.1)	54.1 (15.6)	78 (16.1)
	Med % change		4.9	19.1		7.9	41.3
Medial		112.3 (54.4)	94.1 (58.7)	14 (11.9)	90.7 (5.2)	91 (7.4)	90.3 (5.7)
	Med % change		4.3	-59.8		3.5	-0.1
Anterior		41 (17.1)	53 (14.2)	42 (35)	120.9 (9.8)	125.2 (11.7)	103.2 (12.8)
	Med % change		13.7	2.5		4.2	-10.6